Concentrated Plasticity Elements

The objective in this document is to explain nonlinear frame elements with concentrated plastic hinges at the element ends. These elements contrast with the distributed plasticity elements that are labelled Element 12 (displacement-based) and Element 13 (force-based) in the G2 implementations on this website, covered in another document. As explained by Filippou and Fenves in their 2004 chapter in Bozorgnia and Bertero's book Methods of Analysis for Earthquake-Resistant Structures, there are several ways of formulating concentrated plasticity elements. The categorization of approaches adopted in this document is visualized in Figure 1, with element numbering from G2. Each element type is given on section in the following.

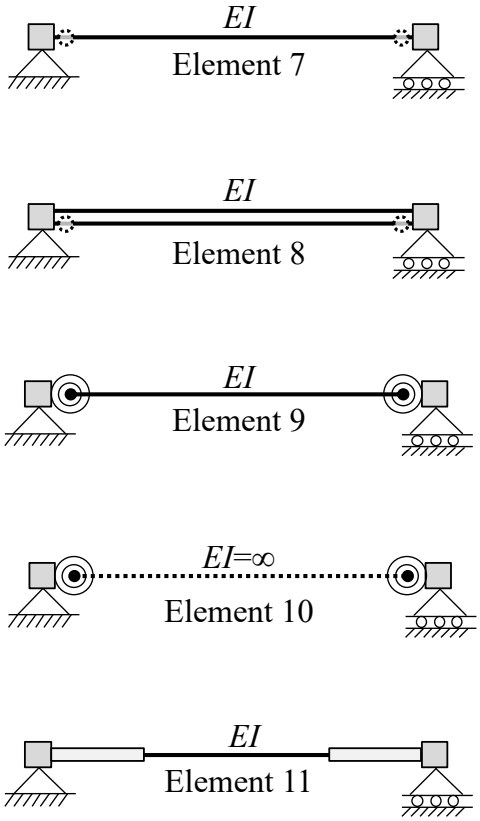

Figure 1: Concentrated plasticity elements.

Element 7: Elastic Perfectly Plastic

This element, shown at the top of Figure 1, has a linear elastic interior, with perfectly plastic hinges forming at the element ends. This means that the bending stiffness at an element end disappears once yielding takes place there. This also means that the structure becomes unstable, with zero stiffness along a mechanism, once a sufficient number of hinges have formed. In other words, there is no hardening. As for any element, the state determination starts with trial global displacements, $\mathbf{u}_g$, given to the element from the

Newton-Raphson algorithm, straightforwardly transformed into basic deformations, $\mathbf{u}_b$, by the kinematic compatibility relationship $\mathbf{u}_b=\mathbf{T}_{bg}\mathbf{u}_g$. Next, the state determination proceeds to the possibility that there is no yielding, in which case the basic forces are

$$\mathbf{F}_b = \mathbf{K}_{b,elastic}\mathbf{u}_b \tag{1}$$

where

$$\mathbf{K}_{b,elastic} = \begin{bmatrix} \frac{4EI}{L} & \frac{2EI}{L} \\ \frac{2EI}{L} & \frac{4EI}{L} \end{bmatrix} \tag{2}$$

That stiffness matrix is usually amended with an extra row and an extra column, containing the axial stiffness EA/L on the diagonal. To assist the explanations, the two end moments in the vector $\mathbf{F}_b$ are denoted by M_{left} and M_{right}. Those moments are compared with the yield moment, M_u, given by the user. In contrast with the fibre-discretized distributed plasticity elements, the user should employ an axial-moment interaction diagram when determining M_u. That typically entails conducting a single initial linear elastic analysis of the structure in order to determine axial forces in the relevant members. That is followed by the reading of M_u from the interaction diagram for the determined axial force value. The comparison of moment values with M_u proceeds as follows: If the absolute value of M_{left} is greater than the absolute value of M_{right} and also greater than M_u then there is yielding at the left end, at the very least. If there is yielding only there, then the stiffness after yielding is, by static condensation,

$$\mathbf{K}_{b,yield\ left} = \begin{bmatrix} 0 & 0 \\ 0 & \frac{3EI}{L} \end{bmatrix} \tag{3}$$

In order to determine the element forces in that case, consider Figure 2. The quantity η_{left} is called an "event factor" and defined as the ratio M_u/M_{left}, i.e., a number less than unity. Because the moment at yielding is $\eta_{left}M_{left}$, the displacement at yielding is $\eta_{left}\mathbf{u}$, where $\mathbf{u}$ is the trial displacements given by the Newton-Rapshon algorithm.

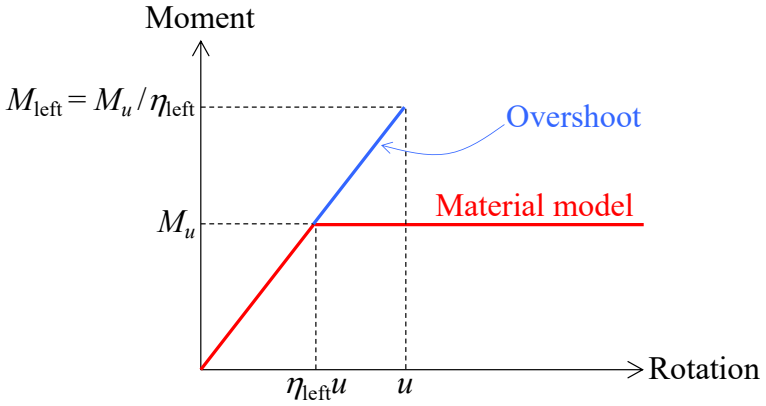

Figure 2: First event factor, at left-hand side yielding.

Up to yielding, the stiffness is given by Eq. (2); after yielding the stiffness is given by Eq. (3). Those two response regimes are captured by the following calculation of the element forces:

$$\mathbf{F}_\text{b} = \eta_\text{left} \cdot \begin{bmatrix} \frac{4EI}{L} & \frac{2EI}{L} \\ \frac{2EI}{L} & \frac{4EI}{L} \end{bmatrix} \mathbf{u}_\text{b} + (1-\eta_\text{left}) \cdot \begin{bmatrix} 0 & 0 \\ 0 & \frac{3EI}{L} \end{bmatrix} \mathbf{u}_\text{b} \tag{4}$$

The absolute value of the moment M_right in that force vector is now compared with M_u. If M_right is larger, then there is yielding also on the right-hand side. In that case, an event factor is again calculated. However, care must be exercised in order to get η_right right. Consider Figure 3, which shows with a black solid dot the moved origin of the moment-rotation plane. In other words, the point at which yielding occurred on the left-hand side is now considered the starting point for the second-slope $3EI/L$ stiffness. To that end, the second event factor is

$$\eta_\text{right} = \frac{M_u - M_\text{right when left yielded}}{M_\text{right} - M_\text{right when left yielded}} \tag{5}$$

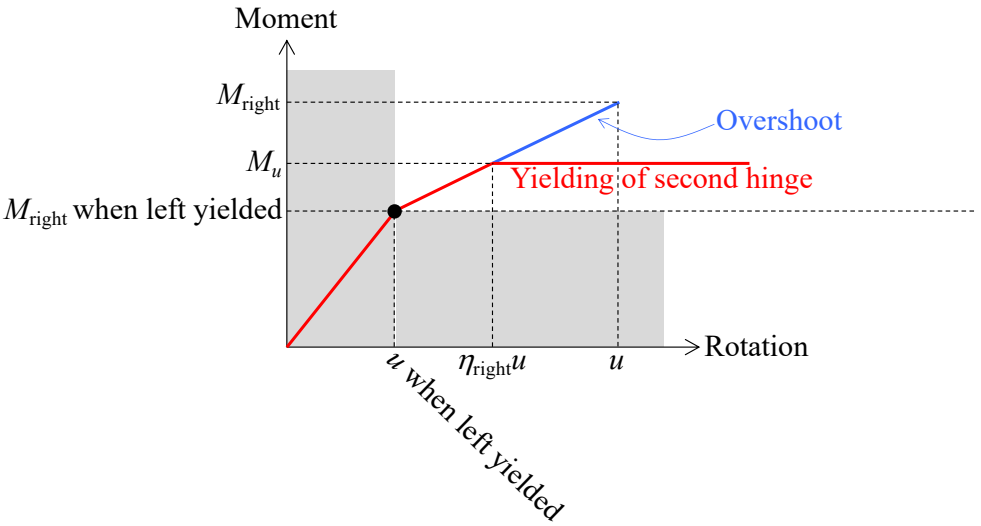

Figure 3: Second event factor, at right-hand side yielding.

The basic forces are then

$$\mathbf{F}_\text{b} = \eta_\text{left} \cdot \begin{bmatrix} \frac{4EI}{L} & \frac{2EI}{L} \\ \frac{2EI}{L} & \frac{4EI}{L} \end{bmatrix} \mathbf{u}_\text{b} + (1-\eta_\text{left}) \cdot \eta_\text{right} \cdot \begin{bmatrix} 0 & 0 \\ 0 & \frac{3EI}{L} \end{bmatrix} \mathbf{u}_\text{b} + (1-\eta_\text{left}) \cdot (1-\eta_\text{right}) \cdot \begin{bmatrix} 0 & 0 \\ 0 & 0 \end{bmatrix} \mathbf{u}_\text{b} \tag{6}$$

where the last term is included here, although the bending stiffness is zero after the last yielding, because the stiffness matrix may include a non-zero axial stiffness term. If the if-statement at the beginning of these explanations revealed that the absolute value of

M_{right} is greater than the absolute value of M_{left}, and also greater than M_u, then the stiffness in the response regime that follows yielding is

$$\mathbf{K}_{\text{b,yield right}} = \begin{bmatrix} \frac{3EI}{L} & 0 \\ 0 & 0 \end{bmatrix} \tag{7}$$

If there is no yielding at all, then it is simply Eqs. (1) and (2) that are returned from the state determination. The state determination here works for "total displacement" situations without cyclic loading. To accommodate cyclic loading, it is necessary to commit the element state upon convergence of the Newton-Raphson iterations, and working with incremental displacements instead of the total displacement.

Element 8: Two-component Parallel System

Another way of formulating an element with concentrated hinges is to consider the degrees of freedom (DOFs) at the element ends to be connected in parallel to the DOFs of the internal components. This approach is schematically shown in Figure 4. At the top of the figure is a generic set of springs to explain the following tenets of any parallel system:

- The system displacement equals the component displacements: $u = u_1 = u_2$
- The system force is the sum of the component forces: $F = F_1 + F_2$
- The system stiffness is the sum of the component stiffnesses:
  $F = F_1 + F_2 = K_1 u_1 + K_2 u_2 = (K_1 + K_2)\, u$

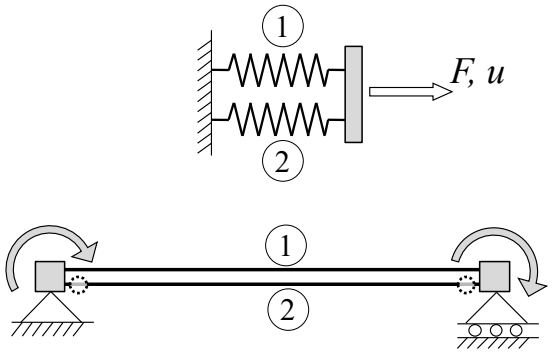

Figure 4: Parallel system.

The actual two-component parallel system model for the element with concentrated hinges is shown at the bottom of Figure 4. The two solid black lines represent two sub-components. The top sub-component is simply linear elastic. The bottom sub-component is also linear elastic in the interior, but the ends follow an elasto-plastic material law. That means they go into yielding once the rotation is sufficiently high. The moment-rotation relationships at either end of those two sub-components are shown in Figure 5, where α is the hardening parameter. For the combined moment-relationship at the top of the figure to be true, the following two conditions apply: 1) The stiffness of the Component 1 must be α times the elastic stiffness; 2) The initial stiffness of Component 2 must be $(1-\alpha)$ times the elastic stiffness.

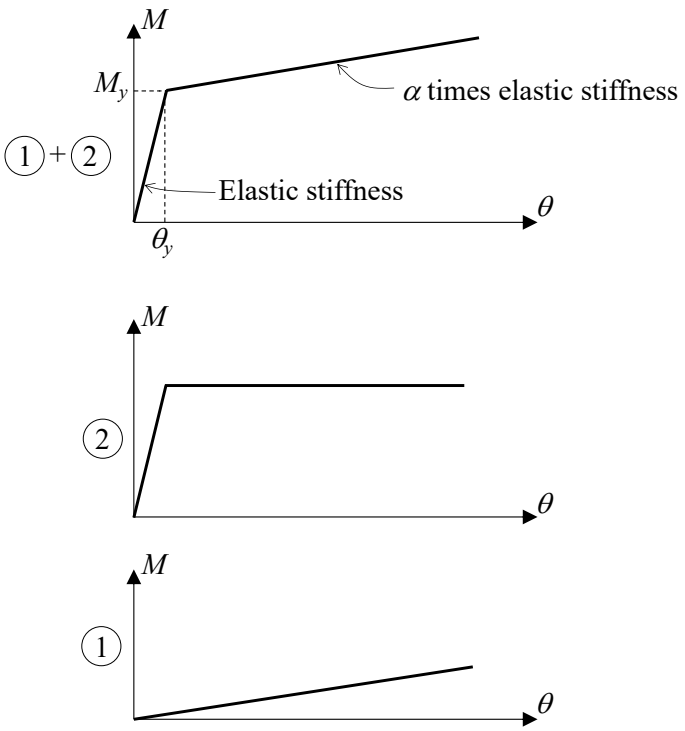

Figure 5: Moment-rotation relationships for parallel model.

With those material models, the force-deformation relationship, $\mathbf{F}_b=\mathbf{K}_b\mathbf{u}_b$, for the two-component element in Figure 4, is obtained by adding stiffness matrices. Four cases must be formulated, in order to cover all possible states of yielding. In the equations below, the stiffness contribution from Component 1 is consistently written first. First, the case of no yielding at either end of Component 2:

$$\mathbf{F}_b = \left(\alpha \begin{bmatrix} \frac{4EI}{L} & \frac{2EI}{L} \\ \frac{2EI}{L} & \frac{4EI}{L} \end{bmatrix} + (1-\alpha) \begin{bmatrix} \frac{4EI}{L} & \frac{2EI}{L} \\ \frac{2EI}{L} & \frac{4EI}{L} \end{bmatrix} \right) \mathbf{u}_b \tag{8}$$

Second, the case of yielding at the left-hand end of Component 2:

$$\mathbf{F}_b = \left(\alpha \begin{bmatrix} \frac{4EI}{L} & \frac{2EI}{L} \\ \frac{2EI}{L} & \frac{4EI}{L} \end{bmatrix} + (1-\alpha) \begin{bmatrix} 0 & 0 \\ 0 & \frac{3EI}{L} \end{bmatrix} \right) \mathbf{u}_b \tag{9}$$

Third, the case of yielding at the right-hand end of Component 2:

$$\mathbf{F}_b = \left(\alpha \begin{bmatrix} \frac{4EI}{L} & \frac{2EI}{L} \\ \frac{2EI}{L} & \frac{4EI}{L} \end{bmatrix} + (1-\alpha) \begin{bmatrix} \frac{3EI}{L} & 0 \\ 0 & 0 \end{bmatrix} \right) \mathbf{u}_b \tag{10}$$

Fourth, the case of yielding at both ends of Component 2:

$$\mathbf{F}_b = \left(\alpha \begin{bmatrix} \frac{4EI}{L} & \frac{2EI}{L} \\ \frac{2EI}{L} & \frac{4EI}{L} \end{bmatrix} \right) \mathbf{u}_b \tag{11}$$

Suppose the yield moment, M_y, is known. Then the following statements are reflected in the G2 code for Element 8, posted on this website: The stiffness of the elastic element (Component 1) must be $\alpha\ M_y/\theta_y$. The initial stiffness of the elasto-plastic element (Component 2) must be $(1-\alpha)\ M_y/\theta_y$. The elasto-plastic element (Component 2) must yield at moment $(1-\alpha)\ M_y$.

Element 9: One-component Series System

In the series system approach for formulating an element with concentrated yielding, one can identify three components, as illustrated in Figure 6:

- Left-hand side concentrated moment-rotation spring (Component 1)
- Elastic interior beam element (Component 2)
- Right-hand side concentrated moment-rotation spring (Component 3)

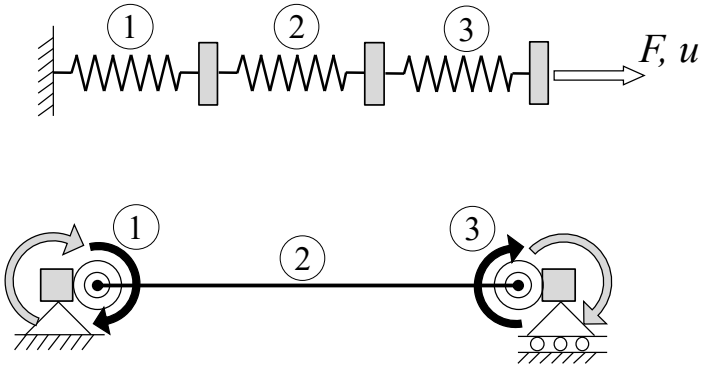

Figure 6: Series system.

At the top of that figure is a generic set of springs to explain the following tenets of any series system:

- The system force equals the component forces: $F = F_1 = F_2 = F_3$
- The system displacement is the sum of the component displacements: $u=u_1+u_2+u_3$
- The system flexibility is the sum of the component flexibilities:
  $u = u_1 + u_2 + u_3 = f_1F_1 + f_2F_2 + f_3F_3 = (f_1 + f_2 + f_3)\ F$

As a result, the formulation of force-deformation relationships in this approach implies adding flexibility matrices, instead of stiffness matrices as above. The result is a two-by-two flexibility matrix, but it can be established by considering four component degrees of freedom:

1. Moment/rotation in left-hand side spring
2. Moment/rotation at left end of elastic beam element

3. Moment/rotation at right end of elastic beam element
4. Moment/rotation in right-hand side spring

The flexibility matrix for those four DOFs is

$$\mathbf{f}_c = \begin{bmatrix} f_{left} & 0 & 0 & 0 \\ 0 & \frac{L}{3EI} & -\frac{L}{6EI} & 0 \\ 0 & -\frac{L}{6EI} & \frac{L}{3EI} & 0 \\ 0 & 0 & 0 & f_{right} \end{bmatrix} \tag{12}$$

where f_{left}=flexibility of the left-hand side spring and f_{right}=flexibility of the right-hand side spring. The equilibrium matrix $\tilde{\mathbf{T}}$, i.e., the counterpart to the kinematic matrix **T**, but for equilibrium, connects the four component forces to the two basic element forces:

$$\tilde{\mathbf{F}}_c = \tilde{\mathbf{T}}_{cb}\tilde{\mathbf{F}}_b = \begin{bmatrix} 1 & 0 \\ 1 & 0 \\ 0 & 1 \\ 0 & 1 \end{bmatrix} \tilde{\mathbf{F}}_b \tag{13}$$

where $\mathbf{F}_c$ are the four component forces listed above. The flexibility matrix for the "final basic configuration" is then

$$\mathbf{f}_b = \tilde{\mathbf{T}}_{cb}^{\mathrm{T}} \mathbf{f}_c \tilde{\mathbf{T}}_{cb} = \begin{bmatrix} \frac{L}{3EI} + f_{left} & -\frac{L}{6EI} \\ -\frac{L}{6EI} & \frac{L}{3EI} + f_{right} \end{bmatrix} \tag{14}$$

The inverse of $\mathbf{f}_b$ when f_{left}=f_{right}=0 is the ordinary Basic stiffness matrix with $4EI/L$ on the diagonal and $2EI/L$ on the off-diagonal; otherwise, it contains slightly more complex expressions.

State Determination for "Force-based" Element

The state determination for Element 9 is conceptually similar to the state determination for the distributed plasticity element labelled Element 13 in the Python code G2 posted on this website. Both are "force-based elements," epitomized in the relationship $\tilde{\mathbf{F}}_{\mathrm{c}} = \tilde{\mathbf{T}}_{\mathrm{cb}}\tilde{\mathbf{F}}_{\mathrm{b}}$ in Eq. (13) and equivalently in the relationship $\tilde{\mathbf{F}}_{\mathrm{springs}} = \tilde{\mathbf{T}}_{\mathrm{springs-basic}}\tilde{\mathbf{F}}_{\mathrm{basic}}$, which gives the force in the springs from the Basic element forces. This relationship does *not* appear in the displacement-based stiffness methods, where the transformation matrices always express "deformations below are equal to the transformation matrix times the deformations above" and in that paradigm, as a result: "forces above are equal to the transformation matrix transposed times the forces below." In force-based elements, where the flexibility matrix will appear, matters are exactly opposite: "forces below are equal to the transformation matrix (the one with a tilde) times the forces above" and as a result: "deformations above are equal to the transformation matrix (the one with a tilde) transposed times the deformations below." This force-based state determination, in the face of a top-level Newton-Raphson algorithm that is conducting equilibrium iterations

for a standard displacement-based finite element code, is illustrated in Figure 7. Because of the force-based approach inherent in the series system implementation of Element 9, we cannot go downwards on the right-hand side. Instead, we must go downwards on the left-hand side, i.e., the equilibrium side. For nonlinear material models, this requires iterations, as is described also in the document on distributed plasticity elements for Element 13. With reference to Figure 7, *compatibility iterations* take place at the element level in order to determine the forces $\tilde{\mathbf{F}}_\mathrm{b}$ that satisfy the following compatibility equations:

$$\mathbf{u}_\mathrm{b}^\mathrm{input} - \mathbf{u}_\mathrm{b}\left(\tilde{\mathbf{F}}_\mathrm{b}\right) = \mathbf{0} \tag{15}$$

For every compatibility iteration, the following force transformation is employed in order to determine the force in the springs:

$$\tilde{\mathbf{F}}_\mathrm{springs} = \tilde{\mathbf{T}}_{\mathrm{springs-Basic}}\tilde{\mathbf{F}}_\mathrm{b} \tag{16}$$

Once the spring receives that force, *equilibrium iterations* take place in the springs in order to determine the deformations $\mathbf{u}_\mathrm{springs}$ that satisfy the following equilibrium equations:

$$\tilde{\mathbf{F}}_\mathrm{springs}^\mathrm{input} - \tilde{\mathbf{F}}_\mathrm{springs}\left(\mathbf{u}_\mathrm{springs}\right) = \mathbf{0} \tag{17}$$

For every equilibrium iteration, the spring deformations are sent to the material model for the springs, if they are modelled by a dedicated material model. See Element 9 in the G2 code posted on this website for further details on the implementation.

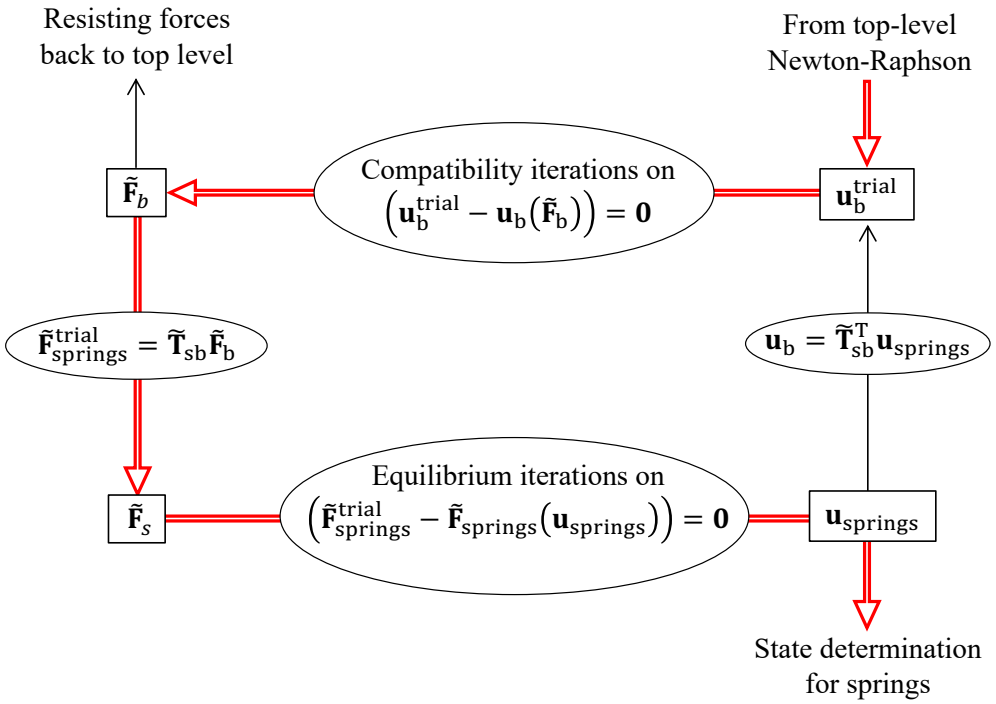

Figure 7: State determination for series system model.

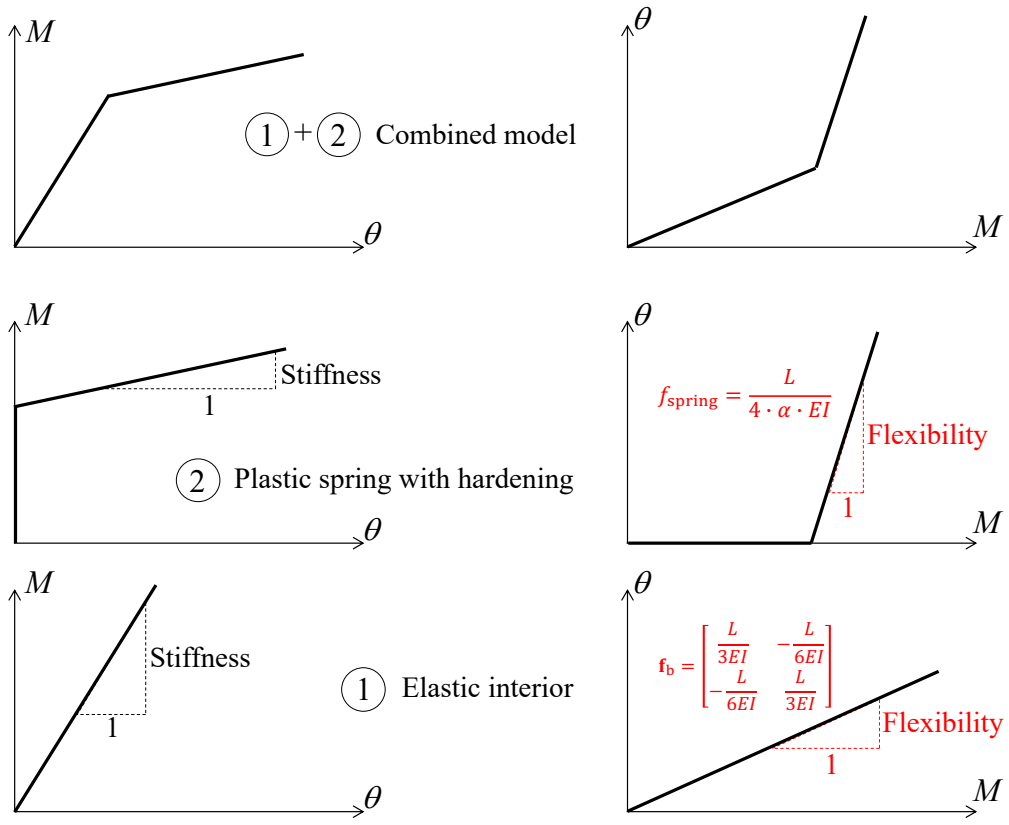

Figure 8: Summation of flexibilities in series system model.

At present, Element 9 is implemented in G2 with a bilinear uniaxial material model as springs. Another, perhaps simpler option, would be to introduce a constant spring flexibility, with hardening parameter denoted by α, as earlier in this document. This model is illustrated in Figure 8, leading to the following algorithm for the compatibility iterations, without equilibrium iterations:

1. Define flexibility matrices:

$$\mathbf{f}_{\text{b,elastic}} = \begin{bmatrix} \frac{L}{3EI} & -\frac{L}{6EI} \\ -\frac{L}{6EI} & \frac{L}{3EI} \end{bmatrix}, \quad \mathbf{f}_{\text{b,plastic 1}} = \begin{bmatrix} \frac{L}{\alpha \cdot 4EI} & 0 \\ 0 & 0 \end{bmatrix}, \quad \mathbf{f}_{\text{b,plastic 2}} = \begin{bmatrix} 0 & 0 \\ 0 & \frac{L}{\alpha \cdot 4EI} \end{bmatrix}$$

2. Initialize element forces, $\mathbf{F}_{\text{b}}$
3. Start Newton-Raphson iterations to enforce the compatibility in the top-most oval in Figure 7
    a. Let the residual element deformations be the total element deformations
    b. Check if any of the springs are yielding for the current value of $\mathbf{F}_{\text{b}}$
    c. Calculate the corresponding deformations, $\mathbf{u}_{\text{b}}$, not by equilibrium iterations, as is done in Element 9b and Element 13 in G2, but by:

$$\mathbf{u}_{\text{b}} = \mathbf{f}_{\text{elastic}}\mathbf{F}_{\text{b,0}} + \mathbf{f}_{\text{b,plastic 1}}\mathbf{F}_{\text{b,1}} + \mathbf{f}_{\text{b,1}}\mathbf{F}_{\text{b}}$$

where $\mathbf{F}_{\text{b,i}}$ are the portions of the element forces up to first yielding, then up to second yielding, etc.

d. Calculate the flexibility matrix for incremental force changes at the current state; for example, after yielding of spring 1, $\mathbf{f}_\mathrm{b} = \mathbf{f}_\mathrm{elastic} + \mathbf{f}_\mathrm{b,plastic\ 1}$
e. Subtract $\mathbf{u}_\mathrm{b}$ from the residual deformations in item a. above
f. Check the norm of the deformation residual; if it is not zero then add $\mathbf{f}_\mathrm{b}^{-1}\boldsymbol{u}_\mathrm{b,residual}$ to $\mathbf{F}_\mathrm{b}$ and go back to item a. above

4. After convergence, the element forces to be returned to the top-level Newton-Raphson algorithm is $\mathbf{F}_\mathrm{b}$ and the corresponding stiffness is $\mathbf{f}_\mathrm{b}^{-1}$.

A drawback of that implementation is that, for cyclic loading, the force-displacement curve appears as shown on the left-hand side of Figure 9. In other words, the above modelling of the plastic response is not hysteretic. This is rectified in the present implementation of Element 9 in G2, posted on this website, where a uniaxial material models the moment-rotation relationship of each hinge. The right-hand side in Figure 9 shows how that leads to a proper hysteretic response, here with kinematic hardening demonstrated for a portal frame subjected to lateral load.

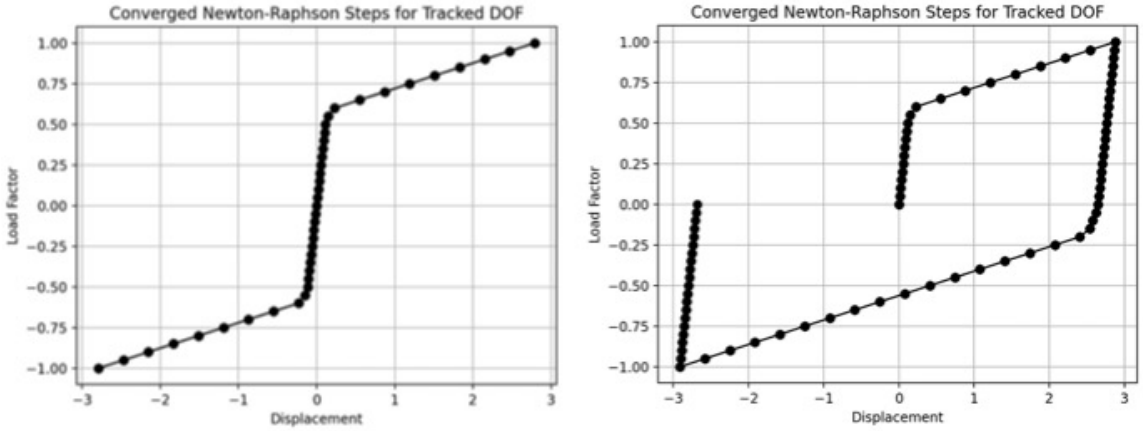

Figure 9: Cyclic response from with different implementations of Element 9.

Element 10: Rigid Interior

Suppose the interior of the element remains rigid, like a stick model, with all deformation concentrated in the end springs. In that case, a uniaxial material model can be employed to model the moment-rotation relationship in each hinge. The state determination starts with the determination of end rotations:

$$\mathbf{u}_b = \mathbf{T}_{bg}\mathbf{u}_g \tag{18}$$

Thereafter, the moment for the given rotation is determined by each uniaxial material model. Finally, the end forces are passed back up to the Newton-Raphson algorithm:

$$\tilde{\mathbf{F}}_g = \mathbf{T}_{bg}^\mathrm{T}\tilde{\mathbf{F}}_b \tag{19}$$

The simplicity of this approach stems from the fact that the interior of the element remains rigid. This is implemented as Element 10 in the G2 code posted on this website.

Calibration of Springs

An important task in the adaptation of concentrated plasticity elements is to calibrate the material law of the springs at the element ends. A natural starting point is computational analysis of the cross-section. Specifically, moment-curvature diagrams are obtained by applying section deformations and observing the evolution of the bending moment. An idealized version of such results is shown at the top of Figure 10. A bi-linear moment-curvature relationship is postulated here, with initial stiffness EI and second-slope stiffness αEI. The question is: What is the corresponding moment-rotation relationship? We seek the yield rotation, the initial stiffness, and the second-slope stiffness of the blue curve at the bottom of Figure 10.

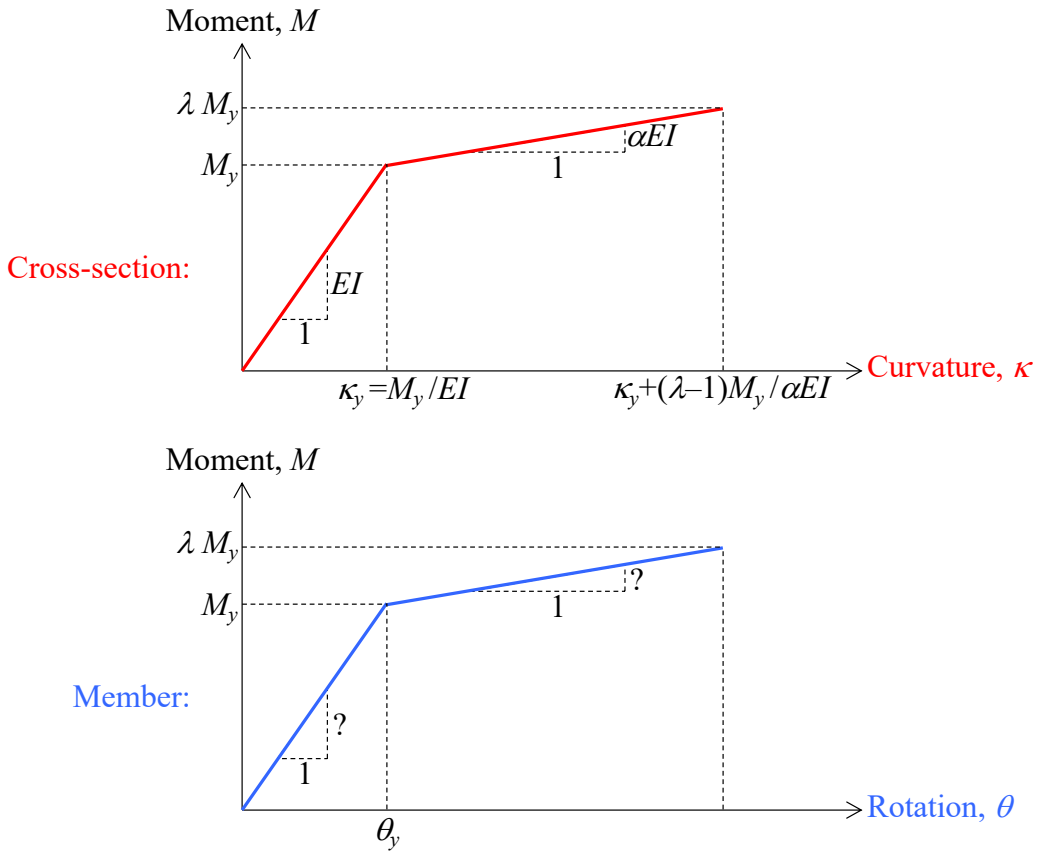

Figure 10: Curvature vs. rotation.

In order to address the aforementioned questions, consider Figure 11. It shows an anti-symmetric bending moment diagram applied to a member in its Basic configuration. Adopting this variation in the bending moment along the element is appropriate when we think of having one element per member. Conversely, a constant (symmetric) bending moment diagram would be appropriate if we think of discretizing the member into many elements. In the top half of Figure 11, end moments equal to the yield moment of the cross-section, M_y, are applied to the member. The structure remains linear elastic; hence, the curvature is just reaching the yield curvature, κ_y, at the member ends. Quick integration with the principle of virtual forces, from elementary structural analysis, suggests that the end rotations are $\theta = M_y L / 6EI$ in this situation. In other words, the initial

slope of the blue line at the bottom of Figure 10 is $6EI/L$. Next, the end moments are increased to λM_y, with λ simply serving as a load factor, with value greater than unity. The bottom portion of Figure 11 illustrates the distribution of curvature along the member in this situation. Because the bending moment values near the member ends exceed M_y, there is concentrated curvature there, as illustrated in Figure 11 and resulting from the moment-curvature diagram in Figure 10. Integration of curvature equals rotation. That is why the area of the "protruding" plastic curvature is the plastic rotation, as indicated in Figure 11.

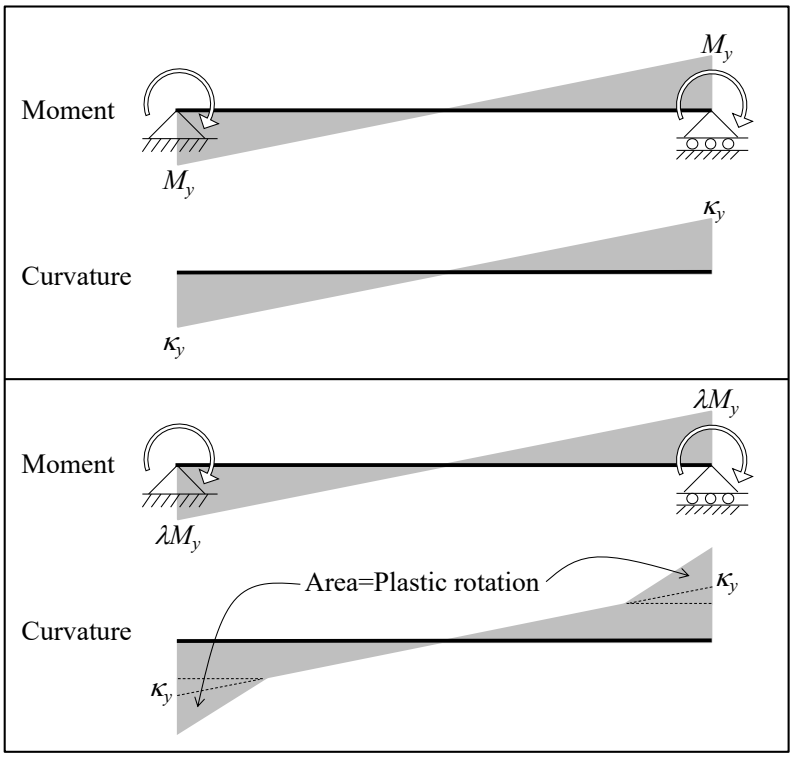

Figure 11: Determination of plastic rotation.

In order to determine the plastic rotation, the curvature is expressed as a function of the bending moment, here for the elastic region:

$$\kappa(x) = \frac{M(x)}{EI} \tag{20}$$

and here for the plastic region, in which $M>M_y$ and $\lambda>1$:

$$\kappa(x) = \frac{M_y}{EI} + \frac{\left(M(x) - M_y\right)}{\alpha \cdot EI} \tag{21}$$

The variation of the bending moment is, in each half of the member:

$$M(x) = \lambda M_y \frac{x}{(L/2)} \tag{22}$$

Equating $M(x)$ with M_y gives the location where the bending moment reaches yield:

$$x = \frac{L}{2\lambda} \tag{23}$$

That means the plastic hinge length is

$$L_p = \frac{L}{2} - \frac{L}{2\lambda} = \frac{L}{2} \cdot \left(1 - \frac{1}{\lambda}\right) \tag{24}$$

Eq. (24) correctly suggests that the plastic hinge length is zero when λ=1. Eq. (24) also shows that the plastic hinge length increases as λ increases, naturally with limiting value $L/2$, which means yielding along the entire member. Next, the expression for the bending moment from Eq. (22) is substituted into the expression of the variation of curvature along the member in the plastic region from Eq. (21), which gives

$$\kappa(x) = \frac{M_y}{EI} + \frac{M_y \cdot \left(\frac{2\lambda x}{L} - 1\right)}{\alpha \cdot EI} \tag{25}$$

The plastic rotation is the area outside the elastic curvature, i.e., the area of the "protruding" plastic curvature triangle at the bottom of Figure 11. The height of that triangle is obtained by evaluating Eq. (25) at $x=L/2$ and ignoring the first term, which gives

$$\kappa_{p,\text{end}} = \frac{M_y \cdot (\lambda - 1)}{\alpha \cdot EI} \tag{26}$$

The length of the aforementioned triangle is the plastic hinge length, L_p. The area of the triangle is the plastic rotation:

$$\theta_p = \frac{M_y \cdot L}{4 \cdot \alpha EI} \cdot \frac{(\lambda - 1)^2}{\lambda} \tag{27}$$

Eq. (27) correctly suggests that the plastic hinge rotation is zero when λ=1 and that the plastic rotation increases in value as λ increases. Because of the presence of λ, Eq. (27) also gives the second-slope stiffness of the blue line in Figure 10, in the sense that the end moments are defined by λ and M_y. However, the blue line in Figure 10 is linear, while Eq. (27) is nonlinear. As is understood from earlier, a bi-linear moment-rotation relationship is sought in this document. One approach to achieve this is to evaluate θ_p in Eq. (27) for two λ-values and draw a line between. The slope of that line is then the *inverse* of the sought λ-θ slope. That approach is adopted here by letting the first λ-value be unity, giving, θ_p=0, and the second simply set equal to λ. The slope of the rotation-

moment relationship is then the difference between the two plastic rotations, divided by the interval in between, which is λ–1:

$$\frac{1}{k_p} = \frac{\theta_p(\lambda)}{\lambda - 1} = \frac{M_y \cdot L}{4 \cdot \alpha EI} \cdot \frac{\lambda - 1}{\lambda} \tag{28}$$

The second column in Table 1 shows the value of the multiplier $\lambda/(\lambda–1)$ that gives k_p in the relationship $M=k_p\theta_p$, with $k_p=multiplier \cdot 4\alpha EI/(M_yL)$, for different values of λ. It shows that the plastic portion of the second-slope stiffness of the blue line in Figure 10 diminishes with increasing reference value of λ. In fact, the large multiplier values that appear for small λ-values indicates a high plastic portion of the second-slope stiffness immediately after yielding. Conversely, when the reference end moments reach twice the yield moment, then the plastic portion of the second-slope moment-rotation stiffness is $8\alpha EI/(M_yL)$. The third column in Table 1 shows the plastic hinge length, calculated from Eq. (24).

Table 1: Second-slope stiffness of the moment-rotation relationship from reference moment.

λ	Multiplier of $\frac{4 \cdot \alpha EI}{M_y \cdot L}$ to obtain k_p	Plastic hinge length, L_p, as fraction of total member length, L
1.05	21.00	0.024
1.1	11.00	0.045
1.15	7.67	0.065
1.2	6.00	0.083
1.25	5.00	0.100
1.3	4.33	0.115
1.35	3.86	0.130
1.4	3.50	0.143
1.45	3.22	0.155
1.5	3.00	0.167
1.55	2.82	0.177
1.6	2.67	0.188
1.65	2.54	0.197
1.7	2.43	0.206
1.75	2.33	0.214
1.8	2.25	0.222
1.85	2.18	0.230
1.9	2.11	0.237
1.95	2.05	0.244
2	2.00	0.250